



# Engagement of cortico-cortical and cortico-subcortical networks in a patient with epileptic spasms: An integrated neurophysiological study

Inoue, Takeshi ; Kobayashi, Katsuya ; Matsumoto, Riki ; Inouchi, Morito ; Togo, Masaya ; Togawa, Jumpei ; Usami, Kiyohide ; Shimotake, Akihiro...

**(Citation)**

Clinical Neurophysiology, 131(9):2255-2264

**(Issue Date)**

2020-09

**(Resource Type)**

journal article

**(Version)**

Accepted Manuscript

**(Rights)**

© 2020 International Federation of Clinical Neurophysiology. Published by Elsevier B.V. All rights reserved.

**(URL)**

<https://hdl.handle.net/20.500.14094/90009370>



Engagement of cortico-cortical and cortico-subcortical networks in a patient with epileptic spasms: An integrated neurophysiological study

Author names and affiliations:

Takeshi Inoue <sup>a,b</sup>, Katsuya Kobayashi <sup>a</sup>, Riki Matsumoto <sup>a,c\*</sup>, Morito Inouchi <sup>d</sup>, Masaya Togo <sup>a</sup>, Jumpei Togawa <sup>a</sup>, Kiyohide Usami <sup>a</sup>, Akihiro Shimotake <sup>e</sup>, Masao Matsushashi <sup>e</sup>, Takayuki Kikuchi <sup>f</sup>, Kazumichi Yoshida <sup>f</sup>, Hisashi Kawawaki <sup>b</sup>, Nobukatsu Sawamoto <sup>a,g</sup>, Takeharu Kunieda <sup>f,h</sup>, Susumu Miyamoto <sup>f</sup>, Ryosuke Takahashi <sup>a</sup>, Akio Ikeda <sup>e\*</sup>

<sup>a</sup> Department of Neurology, Kyoto University Graduate School of Medicine, 54, Shogoin, Sakyo-ku, Kyoto 606-8507, Japan.

<sup>b</sup> Department of Pediatric Neurology, Child and Adolescent Epilepsy Center, Osaka City General Hospital, 2-13-22, Miyakojimahondori, Miyakojima-ku, Osaka, 534-0021, Japan.

<sup>c</sup> Division of Neurology, Kobe University Graduate School of Medicine, 7-5-1 Kusunoki-cho, Chuo-ku, Kobe 650-0017, Japan.

<sup>d</sup> Department of Respiratory Care and Sleep Control Medicine, Kyoto University Graduate School of Medicine, 54, Shogoin, Sakyo-ku, Kyoto

<sup>e</sup> Department of Epilepsy, Movement Disorders and Physiology, Kyoto University Graduate School of Medicine, 54, Shogoin, Sakyo-ku, Kyoto 606-8507, Japan.

<sup>f</sup> Department of Neurosurgery, Kyoto University Graduate School of Medicine, 54, Shogoin, Sakyo-ku, Kyoto 606-8507, Japan.

<sup>g</sup> Department of Human Health Sciences, Kyoto University Graduate School of Medicine, 53, Shogoin, Sakyo-ku, Kyoto 606-8507, Japan.

27 <sup>h</sup> Department of Neurosurgery, Ehime University Graduate School of Medicine,  
28 Shitsukawa Toon City, Ehime 791-0295, Japan.

29

30

31 \* Co-corresponding authors:

32 Riki Matsumoto

33 Division of Neurology, Kobe University Graduate School of Medicine, 7-5-1

34 Kusunoki-cho, Chuo-ku, Kobe 650-0017, Japan.

35 E-mail: matsumot@med.kobe-u.ac.jp

36

37 Akio Ikeda

38 Department of Epilepsy, Movement Disorders and Physiology, Kyoto University

39 Graduate School of Medicine, 54, Shogoin, Sakyo-ku, Kyoto 606-8507, Japan.

40 E-mail: akio@kuhp.kyoto-u.ac.jp

41

42 Author e-mail addresses:

43 inoue@kuhp.kyoto-u.ac.jp (T. Inoue), 31258a@kuhp.kyoto-u.ac.jp (K.  
44 Kobayashi), matsumot@med.kobe-u.ac.jp (R. Matsumoto),  
45 inouchi@kuhp.kyoto-u.ac.jp (M. Inouchi), masat43@kuhp.kyoto-u.ac.jp (M.  
46 Togo), jumpeit@kuhp.kyoto-u.ac.jp (J. Togawa), ukiyo@kuhp.kyoto-u.ac.jp (K.  
47 Usami), smtk@kuhp.kyoto-u.ac.jp (A. Shimotake), matuhasi@kuhp.kyoto-u.ac.jp  
48 (M. Matsubishi), tkik@kuhp.kyoto-u.ac.jp (T. Kikuchi),  
49 kazuy@kuhp.kyoto-u.ac.jp (K. Yoshida), m8919548@msic.med.osaka-cu.ac.jp  
50 (H. Kawawaki), sawa@kuhp.kyoto-u.ac.jp (N. Sawamoto),  
51 kuny@m.ehime-u.ac.jp (T. Kunieda), miy@kuhp.kyoto-u.ac.jp (S. Miyamoto),  
52 ryosuket@kuhp.kyoto-u.ac.jp (R. Takahashi), akio@kuhp.kyoto-u.ac.jp (A.  
53 Ikeda).

54

55 Number of characters in the title: 138 characters

56 Number of words in the abstract: 200 words

57 Manuscript word count: 5,319 words

58 Number of figures: 6

59 Number of supplementary figures: 1

60 Number of tables: 0

61 Conflict of Interest Statement

62           None of the authors have any conflicts of interest or potential financial  
63 interests to disclose.

64           Department of Epilepsy, Movement Disorders and Physiology is the  
65 Industry-Academia Collaboration Courses, supported by Eisai Co., Ltd.,  
66 Nihon Kohden Corporation, Otsuka Pharmaceutical Co., and UCB Japan Co.,  
67 Ltd.

68

69 Acknowledgments

70           We would like to thank Dr. H. Otsubo (Division of Neurology, The  
71 Hospital for Sick Children, Toronto, Canada) for his helpful advice on this  
72 manuscript.

73           This work was supported by the Japan Ministry of Education, Culture,  
74 Sports, Science and Technology (MEXT) KAKENHI [grant numbers 17H05907,  
75 18H02709, 18K19514, 15H05874, 15H05875 and 19H03574]; the Japan Society  
76 for the Promotion of Science (JSPS) KAKENHI [grant number 17K16120]; and a  
77 Research Grant from the Japan Epilepsy Research Foundation.

78

## 79 Abstract

80 **Objective:** We aimed to delineate the engagement of cortico-cortical and  
81 cortico-subcortical networks in the generation of epileptic spasms (ES) using  
82 integrated neurophysiological techniques.

83 **Methods:** Seventeen-year-old male patient with intractable ES underwent  
84 chronic subdural electrode implantation for presurgical evaluation. Networks  
85 were evaluated in ictal periods using high-frequency oscillation (HFO) analysis  
86 and in interictal periods using magnetoencephalography (MEG) and  
87 simultaneous electroencephalography, and functional magnetic resonance  
88 imaging (EEG-fMRI). Cortico-cortical evoked potentials (CCEPs) were recorded  
89 to trace connections among the networks.

90 **Results:** Ictal HFO revealed a network comprising multilobar cortical regions  
91 (frontal, parietal, and temporal), but sparing the positive motor area. Interictally,  
92 MEG and EEG-fMRI revealed spike-and-wave-related activation in these cortical  
93 regions. Analysis of CCEPs provided evidence of connectivity within the  
94 cortico-cortical network. Additionally, EEG-fMRI results indicate the involvement  
95 of subcortical structures, such as bilateral thalamus (predominantly right) and  
96 midbrain.

97 **Conclusions:** In this case study, integrated neurophysiological techniques  
98 provided converging evidence for the involvement of a cortico-cortical network  
99 (sparing the positive motor area) and a cortico-subcortical network in the  
100 generation of ES in the patient.

101 **Significance:** Cortico-cortical and cortico-subcortical pathways, with the  
102 exception of the direct descending corticospinal pathway from the positive motor

103 area, may play important roles in the generation of ES.

## 104 Highlights

- 105 • We applied integrated neurophysiology to investigate epileptic network activity
- 106 during epileptic spasms (ES).
- 107 • Neurophysiological techniques revealed the engagement of cortico-cortical and
- 108 subcortical networks.
- 109 • Pathways other than the direct descending pathway from the positive motor
- 110 area may be important in the generation of ES.

111

## 112 Keywords

113 epileptic spasm; high frequency oscillation; cortico-cortical evoked potential;  
114 EEG with functional MRI (EEG-fMRI)

115

## 116 Abbreviations

117 ES, epileptic spasms; HFO, high-frequency oscillation; EMG, electromyogram;  
118 CCEP, cortico-cortical evoked potential; ECoG, electrocorticogram; EEG-fMRI,  
119 EEG with functional MRI; BOLD, blood-oxygen-level-dependent; PMA, positive  
120 motor area; STFT, short-time Fourier transform; IPL, inferior parietal lobule; CST,  
121 corticospinal tract; CRT, corticoreticular tract; RST, reticulospinal tract.



## 122 Introduction

123       Epileptic spasms (ES) generally consist of brief contractions of axial and  
124 proximal muscles of the extremities, resulting in muscle flexion, extension, or a  
125 mixture of both (Engel, 2001; Vigeveno et al., 2001; Watanabe et al., 2001;  
126 Fisher et al., 2017). In the revised operational classification of seizure types by  
127 the International League Against Epilepsy (ILAE), ES are classified as either  
128 focal, generalized, or of unknown type (Fisher et al., 2017). The precise  
129 mechanisms by which ES are generated remain elusive. However,  
130 cortico-cortical and/or subcortical networks are considered to underlie the  
131 semiology of ES (Chugani et al., 1992, 2015; Ramachandran et al., 2008;  
132 Iimura et al., 2017, 2018).

133       High-frequency oscillations (HFOs), usually defined as oscillations at  
134 frequencies above 80 Hz, are divided into ripples (80–250 Hz) and fast ripples  
135 (FRs; 250–500 Hz) (Bragin et al., 1999; Jacobs et al., 2010; Frauscher et al.,  
136 2017; Zijlmans et al., 2017). Pathological HFOs, especially FRs, represent  
137 abnormal bursts of spike-and-wave populations or action potentials of pyramidal  
138 cells (Le Van Quyen et al., 2007; Bragin et al., 2010; Jiruska et al., 2010, 2017).

139       Based on the results of recent studies, interictal and ictal HFOs are  
140 considered possible biomarkers of epileptogenicity (Ochi et al., 2007; Wu et al.,  
141 2010; Akiyama et al., 2011; Jacobs et al., 2012; Zijlmans et al., 2017). However,  
142 it is difficult to demonstrate an inter-areal connection of networks by analyzing  
143 HFOs alone. In one study on patients with ES, an initial increase in ripple activity  
144 in the primary motor area was reported to occur prior to the changes in  
145 electromyogram (EMG) activity accompanying ES (Nariai et al., 2011). The

146 authors reported that the recruitment of primary motor area neurons into ripple  
147 production may play an important role in the generation of ES. Meanwhile, Iimura  
148 et al. reported extensively distributed interictal HFOs which spared the primary  
149 motor area in patients with intractable ES, requiring subtotal hemispherectomy or  
150 multilobar resection (Iimura et al., 2017). In that particular study, abnormal  
151 cortico-cortical connections in multilobar epileptic zones were considered  
152 possible generators of ES. Therefore, various mechanisms have been proposed  
153 to underlie ES generation and further investigations using different methods are  
154 warranted.

155         In this report, we present a case study of a patient with ES analyzed  
156 using state-of-the-art integrated neurophysiological techniques to delineate the  
157 network involved in ES. The network was evaluated ictally by assessing ictal  
158 HFOs, and interictally with magnetoencephalography (MEG), and simultaneous  
159 electroencephalography and functional MRI recording (EEG-fMRI). An electrical  
160 tract-tracing method using cortico-cortical evoked potentials (CCEPs) was  
161 employed to probe connectivity within the network.

## 2. Methods

### 2.1 Patient information

A 17-year-old, right-handed man was assessed at our institution. The patient started suffering from clusters of ES at 8 months of age. He manifested hypsarrhythmia and psychomotor deterioration, consistent with West syndrome. Treatment with valproic acid resulted in seizure-free state within a month. However, at the age of 1 year and 8 months, the patient relapsed into experiencing ES in clusters, which were brought into remission by additional treatment with clonazepam at the age of 2 years.

At 6 years of age, both valproic acid and clonazepam were discontinued. From the age of 8 years, the patient's EEG frequently showed spike-and-wave pattern in the right frontal area (Fp2, F4), but focal seizures did not occur. He presented with clusters of ES at 15 years of age, with seizures experienced until surgery and persisting after the procedure. His full intelligence quotient was assessed as 94 at 15 years of age, but his cognitive function gradually declined as the seizures increased in frequency and severity. He did not show any motor deficit. ES were refractory to six antiepileptic drugs and one course of adrenocorticotrophic hormone administration. Brain imaging performed using a 3-Tesla MRI showed normal structure, while interictal scalp EEG showed bilateral (generalized) spike-and-waves (1.5-2.5 Hz) with a right hemispheric predominance. Interictal spike-and-wave analysis using MEG revealed three clusters of dipoles in the right frontal, temporal and parietal association cortical regions (Fig. 1A). An F-18 fluorodeoxyglucose positron emission tomography (FDG-PET) scan showed hypometabolism in regions corresponding to the

clusters of MEG dipoles (Fig. 1B). Subtraction ictal single-photon emission computed tomography co-registered to MRI (SISCOM) showed hyperperfusion in the right frontal and temporal lobes. Considering all of the presurgical findings, which were generally concordant but distributed in a multilobar fashion, the clinical team hypothesized that the ES were generated by a distributed network spread over the three lobes and offered a possible surgical treatment using multilobar corticectomy. The patient and his family elected to undergo invasive presurgical evaluations with implantation of subdural electrode grids for two weeks to identify the seizure onset zone or network, as well as the eloquent cortical areas. An EEG-fMRI was performed as part of non-invasive presurgical evaluations and CCEPs were recorded during invasive evaluations. The present study was approved by the Ethics Committee of our institute (Nos. 79, E217, and 443). Written informed consent was obtained from the patient and his parents.

## 2.2 ECoG (electrocorticogram) recording

The patient underwent chronic subdural grid electrode implantation (total 146 electrodes), covering the right hemisphere (Fig. 1C). The electrodes were made of platinum with a recording diameter of 2.3 mm and center-to-center inter-electrode distance of 10.0 mm (Ad-Tech, Racine, WI, USA). Electrocorticogram (ECoG) recording was performed with a bandpass filter of 0.016–600 Hz and a sampling rate of 2,000 Hz (EEG 1200, Nihon Kohden, Tokyo, Japan). Reference measurements were obtained from a scalp electrode placed on the skin over the left mastoid process. EMGs were recorded from the bilateral deltoid muscles. In this study, we employ the term "positive motor area (PMA)" to

refer to the region showing positive motor symptoms during high-frequency (50 Hz) electrical stimulation (Fig. 1C) (Matsumoto et al., 2007, 2012).

### 2.3 Ictal ECoG recording and HFO analysis

During two weeks of ECoG recording, the patient experienced six clusters of ES characterized by the raising of both shoulders with the left side predominating, sometimes accompanied by a brief vocalization. Usually, ictal ECoG changes started with polyspike and waves, which were widely distributed over the multilobar areas (frontal, temporal, and parietal cortices), with relative sparing of the PMA. Alternatively, the seizure onset zone was not localized to a single cortical region, rather distributed over the three lobes. Therefore, these seizure onset zones could be regarded as components of a seizure-onset network. We evaluated ictal HFOs by time-frequency analysis using a short-time Fourier transform (STFT) (Imamura et al., 2011; Kanazawa et al., 2015; Kobayashi et al., 2017). We analyzed the first ES from each of the six clusters, since the distribution of HFOs became widely distributed as the ES repeated. In doing this, our aim was to focus on the initial change accompanying ES. HFOs were defined by fast oscillatory activity, with a frequency higher than 80 Hz. They were visually identified as discrete and sustained band-like power elevations that were clearly distinguished from the preictal baseline state in the STFT analysis. Additionally, we evaluated HFOs by visual inspection and excluded sharp transients (epileptic spike-and-wave patterns or artifacts) and signals with harmonics from the ECoG trace (Benar et al., 2010; Amiri et al., 2016). The onset of EMG changes occurring in the left deltoid muscle was set as the reference

time point (0 s). The STFT was performed at each time-step on a window covering 40 data points (20 ms; frequency resolution, 10 Hz). The time-step of the sliding window was set to 10 ms. The spectral power ( $\mu\text{V}^2$ ) was calculated every 50 Hz, and its logarithmic power spectrum (base 10) was computed for the given frequency range and window. The baseline was set as the period from -2.5 to -1.5 s relative to EMG onset, to avoid any influence of the initial ES-induced change. To evaluate the power distribution of HFOs, we analyzed the logarithmic power changes in the ripple band (80–250 Hz) from -2.5 to -1.5 s relative to the initial EMG change for each of the first ES. We classified the electrode recording sites using anatomical and functional criteria as follows: PMA (18 electrodes) and outside the PMA (non-PMA; frontal: 60 electrodes, temporal: 40 electrodes, parietal: 28 electrodes). The maximal power of each electrode was calculated. Next, we quantified the time at which the magnitude of the initial EMG change exceeded three standard deviations (SD) above baseline and compared times between the four areas. Ictal HFO and CCEP (see below) analyses were performed on the data offline using in-house scripts (developed by M.M.) for MATLAB (Version 8.1.0; Math Works Inc., Natick, Massachusetts, USA). The Wilcoxon signed-rank test with correction for multiple comparisons was used to compare the differences between signals from F, P, T, and the PMA. The significance level was set at  $p < 0.05$ .

## 2.4 CCEP data acquisition

We investigated inter-areal connections between areas with CCEPs using the methods described previously (Matsumoto et al., 2004, 2012, 2017). In

258 brief, repetitive electrical stimulation was applied in a bipolar manner to a pair of  
259 adjacently placed subdural electrodes using a constant-current stimulator  
260 (MEE-1232, Nihon Kohden, Tokyo, Japan). Single-pulse electrical stimuli  
261 (square-wave pulse: 0.3 ms duration; alternating polarity at 1 Hz) were  
262 systematically applied to all of the electrodes necessary to map the epileptic  
263 and/or functional networks. The stimulus intensity was set at 6–10 mA after  
264 confirming the absence of after-discharges and excessive artifacts. Raw ECoG  
265 was recorded using the same settings for ictal HFO analysis, except for the  
266 application of a bandpass filter of 0.08–600 Hz. CCEPs were obtained offline by  
267 averaging the ECoG signal time-locked to the onset of stimulation. Two trials of  
268 30 responses each were averaged to confirm waveform reproducibility. To  
269 delineate the epileptic and/or functional networks, we selected stimulation sites  
270 (pairs of electrodes) within the seizure onset network in the multilobar cortices.

271         Nine pairs of electrodes were located in PMA, and 62 pairs outside PMA  
272 (non-PMA; frontal: 30 pairs, temporal: 18 pairs, parietal: 14 pairs). In the  
273 remaining three pairs, stimulation was delivered at the border, namely, through  
274 one electrode at PMA and another at non-PMA. CCEPs consisted of an early  
275 (N1) and a late (N2) negative potential. N1 is an early, brief, negative component  
276 occurring 10–50 ms after stimulation (Figs. 2A-C). In this study, we focused on  
277 analyzing N1, since this was the potential investigated in previous studies  
278 (Matsumoto et al., 2004, 2007; Keller et al., 2011; Usami et al., 2017). Regarding  
279 the significance of the CCEP responses, we selected N1 as the point at which  
280 the amplitude exceeded the mean + 6 SD from baseline (Keller et al., 2011,  
281 Usami et al., 2017) (Fig. 2C), and defined this as a significant response. The

baseline was set at 0.095 s before the onset of stimulation.

We hypothesized that the multilobar cortico-cortical network is one of the main generators of ES, while PMA does not deeply comprise this multilobar network, namely, the connection from the areas outside PMA (non-PMA) to PMA is less involved. In order to validate this hypothesis, we compared PMA and non-PMA connectivity with its emphasis on the connection to PMA. For this purpose, we defined a index ratio where the number of significant CCEP electrodes at PMA was divided by that at the whole cortical areas covered by the subdural grid. We then compared the index ratio between the two groups of the stimulus sites: PMA stimulation (9 pairs) vs. non-PMA stimulation (62 pairs: 30 pairs, temporal: 18 pairs, parietal: 14 pairs). The Wilcoxon signed-rank test with correction for multiple comparisons was used to compare the differences of the index ratio between the two groups. The significance level was set at  $p < 0.05$ .

## 2.5 EEG-fMRI data acquisition

An EEG-fMRI scan was performed as part of a presurgical evaluation and spike-and-wave-related activation/deactivation was analyzed using a general linear model. The details of the EEG-fMRI method have been described in our previous report (Usami et al., 2016). EEG and fMRI were recorded simultaneously, with all signals transmitted from an MR-compatible amplifier and sampled at 5 kHz (BrainAmp MR plus; Brain Products, Munich, Germany). A 3-Tesla MRI system (Trio; Siemens, Erlangen, Germany) was used for fMRI recording. Interictal epileptiform discharges were visually identified by two certified electroencephalographers (T.I., M.I.; Fig. 3A). The total recording time



306 was 60 min and obtained data were pre-processed and analyzed using the  
307 FMRI Software Library v5.0 (FSL; [www.fmrib.ox.ac.uk/fsl](http://www.fmrib.ox.ac.uk/fsl)). fMRI data sets were  
308 analyzed based on an event-related design using a general linear model  
309 implemented in the FEAT program (part of FSL). For assigning the onsets of  
310 spike-and-wave patterns as events, a series of time-shift models were calculated  
311 in which the hemodynamic response function (HRF) was applied before or after  
312 spike-and-waves ( $t = -8, -6, -4, -2, +2, \text{ or } +4 \text{ s}$ ). Time-series analyses were  
313 performed using FMRI's Improved Linear Model (FILM) with local  
314 autocorrelation correction. The threshold for Z-statistic images were at  $Z > 2.3$  at  
315 the voxel level to identify clusters, and a corrected cluster significance level of  $p$   
316  $< 0.007$  was applied (equal to  $0.05/7$ ; Bonferroni correction was applied to the  
317 statistical comparisons, since seven time-series models were used) (Worsley,  
318 2001; Usami et al., 2016). Images were then coregistered to the anatomical  
319 image of the patient's brain.

### 320 3. Results

#### 321 3.1 Ictal epileptic and/or functional networks revealed by ictal HFOs

322 Based on data from all six clusters of ES, ictal HFOs spanned a wide  
323 range of frequencies and were most prominent in the ripple band (80–120 Hz).  
324 Spatially, ictal HFOs were widely distributed, occurring mainly in the frontal and  
325 parietal lobes (and to some extent in the temporal lobe), initially sparing the PMA.  
326 A representative time-frequency analysis of an ES is shown in Fig. 4. The  
327 spectral power levels in frontal, parietal, and temporal were all significantly  
328 higher than the power in the PMA (Wilcoxon signed-rank test with correction for  
329 multiple comparisons, all  $p < 0.05$ ; Fig. 5A). The timings of frontal, parietal, and  
330 temporal at which the power of the initial EMG change exceeded 3 SD above  
331 baseline, all occurred significantly earlier than those in the PMA (Wilcoxon  
332 signed-rank test with corrections for multiple comparisons, all  $p < 0.05$ ; Fig. 5B).

333

#### 334 3.2 CCEP connectivity within epileptic and/or functional networks

335 CCEPs revealed a bidirectional connection among seizure onset zones  
336 in the frontal, parietal, and temporal lobes, sparing the PMA. The representative  
337 CCEP investigations were shown in Figs. 2A, B and supplementary Figs. 1A, B.  
338 For example, Fig. 2B showed that stimulation of the IPL (one of the seizure onset  
339 zones, included in the resection areas) elicited adjacent CCEP responses in the  
340 IPL and remote CCEP responses in the premotor area (the site of maximal  
341 response) and temporal cortex, relatively sparing the PMA. Stimulation of the  
342 seizure onset zones in the frontal and temporal areas elicited remote CCEP  
343 responses in the other association areas as well, sparing PMA (supplementary

344 Figs 1A, B).

345       Regarding the connectivity to the PMA, stimulation of the PMA (9 pairs)  
346 elicited significant CCEP responses (N1) in  $84.0 \pm 30.9$  (mean  $\pm$  SD) electrodes.  
347 Of these,  $13.6 \pm 2.8$  electrodes were located in the PMA (index ratio of  $16.1 \pm$   
348  $4.8\%$  [mean  $\pm$  SD]). Conversely, stimulation of the non-PMA (62 pairs) elicited  
349 significant responses in  $74.6 \pm 28.1$  electrodes. Of these,  $9.2 \pm 5.7$  electrodes  
350 were located in the PMA (index ratio of  $12.3 \pm 5.9\%$ ). The index ratio was  
351 significantly higher for PMA stimulation than non-PMA stimulation (Wilcoxon  
352 signed-rank test with correction for multiple comparisons,  $p < 0.05$ ) (Fig. 2D).  
353 These results suggest that the PMA has tighter connections to PMA itself  
354 compared with non-PMA.

355

### 356 3.3 Interictal network revealed by EEG-fMRI

357       In total, 228 spike-and-waves were analyzed during 60 min of EEG-fMRI  
358 recording (Fig. 3A). EEG-fMRI analysis revealed spike-and-wave-related  
359 activations (positive BOLD responses) in subcortical structures (right-dominant  
360 bilateral thalamus and the midbrain), as well as in right-dominant bilateral frontal,  
361 temporal, and parietal lobes, sparing the PMA in the -4 to +4 s time-shift models  
362 (Fig. 3B). Activation was also observed in the bilateral cerebellum,  
363 predominantly on the left side. However, deactivations (negative BOLD  
364 responses) were observed in bilateral PMA, superior parietal lobule, and  
365 precuneus with the 0 to +4 s time-shift models.

366

### 367 3.4 Resective surgery, pathology, and seizure outcome

368           Based on the results of clinical and multimodal evaluations, including  
369 ictal and interictal ECoG, brain MRI, and functional brain mapping, surgical  
370 treatment with multilobar corticectomy was proposed, sparing the PMA (Fig. 1C).  
371 After extensive discussion with the patient and his family, the patient underwent  
372 a tailored multilobar corticectomy. The pathological analysis diagnosed focal  
373 cortical dysplasia type 1c (ILAE classification) in the frontal, parietal, and  
374 temporal regions. The patient was initially free from seizures for 8 months  
375 following surgery, but manifested rare seizures afterwards (ILAE class 4).  
376 Clusters became less frequent (pre-surgery: 3–5 series/day; post-surgery: 2–3  
377 series/week) and shorter (pre-surgery: 10–20 min; post-surgery: 3–5 min). After  
378 surgery, the patient was able to return to normal life and continue his education.

## 379 4. Discussion

380 Our results suggest the following: 1) the pattern of ictal HFO signal  
381 power and timings indicates a less intense and delayed involvement of the PMA  
382 in ictal activity, than in other areas; 2) CCEP evaluation revealed multilobar  
383 cortico-cortical connections among seizure onset zones in the association areas,  
384 while these non-PMA area had less connections to PMA compared with the PMA  
385 itself; and 3) spike-and-wave-related activations occurred in the cerebral cortex,  
386 sparing the PMA and the upper brainstem (midbrain), as revealed by EEG-fMRI.  
387 These findings complement each other to provide converging evidence that the  
388 epileptic network spares the PMA (relative to non-PMA) and that subcortical  
389 structures are important in the pathophysiology of ES in this patient.

390

### 391 4.1 Cortical network

392 Iimura et al. proposed several potential mechanisms underlying the  
393 sparing of the primary motor area in patients with drug-resistant epilepsy  
394 undergoing subtotal hemispherectomy or multilobar resections (Iimura et al.,  
395 2017). One potential mechanism is because the primary motor area is already  
396 myelinated before birth, while the association fiber pathways become gradually  
397 myelinated after birth (Flechsig, 1901, Casey et al., 2005, Deoni et al., 2012).  
398 Possibly, epileptiform discharges preferentially spread and synchronize through  
399 fibers that are myelinated to the same degree, namely the association fibers.  
400 This is concurrent with a recent study that focused on fronto-parietal connectivity  
401 (Matsumoto et al., 2012). The study revealed two connectivity frameworks: 1) a  
402 near-to-near and distant-to-distant mirror symmetric configuration across the

central sulcus, and 2) a preserved dorso-ventral organization. Indeed, we observed the second pattern in our present case; namely, the IPL was connected to the ventral premotor area. Since the CCEP, at least the very first volley is conveyed through the direct white matter pathway (Yamao et al., 2014), the cortico-cortical network in our patient likely involved the II and III branches of the superior longitudinal fasciculus. In the present patient, CCEP evaluation demonstrated the multilobar cortico-cortical connections among the seizure onset zones in the association areas, generally sparing the PMA. The coverage of occipital cortex, however, was not sufficient enough to evaluate the occipital involvement. Further studies are needed to delineate the involvement of the occipital cortex in generation of ES.

#### 4.2 Possible involvement of subcortical structures

EEG-fMRI analysis with the time-shift models (-4 to +4 s) revealed spike-and-wave-related activation in subcortical structures (right-dominant thalamus and the midbrain) and the cerebellum. The cerebral cortex receives projections from the basal ganglia and cerebellum via the thalamus. The thalamus has rich connectivity with the cerebral cortex, creating complex cortico-basal and cortico-cerebellar circuits (Morel et al., 1997; Behrens et al., 2003; Catani et al., 2012). The thalamus and cerebellum may be involved in generating and maintaining generalized spike-and-wave / polyspike-and-waves, as reported in idiopathic and symptomatic generalized epilepsy, via the interaction with the cerebral cortex (Avoli et al., 2001; Aghakhani et al., 2004; Gotman et al., 2005; Hamandi et al., 2006; Liu et al., 2008).

In addition to the involvement of the thalamus and cerebellum, our EEG-fMRI results revealed some activation of the midbrain. This is partially consistent with previous EEG-fMRI recordings obtained during hypsarrhythmia in West syndrome, which demonstrated the involvement of subcortical structures such as the brainstem, putamen, and thalamus (Steriade et al., 2002; Aghakhani et al., 2004; Siniatchkin et al., 2007; Japaridze et al., 2013). Moeller et al. proposed that ES result from the intermittent involvement of descending brainstem pathways controlling spinal reflex activity and indicated the importance of subcortical structures in the pathophysiology of ES (Moeller et al., 2013). Our current report presents a single case study and, as such, the EEG-fMRI findings reported here are not necessarily generalizable to ES research as a whole.

#### 4.3 Potential mechanisms of ES generation

There are two main descending pathways from the cerebral cortex to the spinal tracts: the corticospinal tract (CST) and cortico-reticulospinal tract. CST is primarily concerned with the control of voluntary, discrete, and skilled movements, especially those involving the distal parts of the extremities. Conversely, the cortico-reticulospinal tract consists of the corticoreticular tract (CRT) and the reticulospinal tract (RST; Fig. 6D). The CRT is known to originate mainly in the premotor cortex and terminate at the medullary reticular formation. The RST is divided into two pathways: the medial RST originates in the pontine reticular formation, while the dorsal RST originates in the medullary reticular formation. The medial and dorsal RST provide balanced excitatory and inhibitory

descending regulation of the spinal stretch reflex, and activate axial and proximal muscles of the extremities. These pathways are involved in postural control and locomotor function (Kably et al., 1998; Matsuyama et al., 2004; Yeo et al., 2012).

One potential mechanism underlying ES generation in the patient studied may involve abnormal impulses in the premotor cortex carried via the CRT and RST. Some imbalance of the medial and dorsal RST may cause an abnormal activation of axial and proximal muscles of the extremities, leading to ES (Fig. 6D).

Furthermore, high-frequency electrical stimulation of the dorsolateral premotor and supplementary motor areas produces proximal and axial tonic muscle contraction, while that of the primary motor area generally produces clonic muscle contraction (Uematsu et al., 1992; Lüders et al., 2008).

Considering the semiology of ES, the premotor area and its descending tracts (CRT and RST), rather than the primary motor area and CST, could be implicated in generating ES in our patient (Fig. 6D).

Various suggestions for the semiology and mechanisms underlying ES have been proposed, and further studies using different methods need to be performed. In the present case, the patient experienced a relapse of ES eight months after a targeted multilobar corticectomy. This relapse likely resulted from the insufficient disruption of the multilobar networks.

## 5. Conclusions

The present integrated neurophysiological study demonstrated the importance of both cortico-cortical and cortico-subcortical networks in the



475 generation of ES in the patient studied. There may be multiple varied  
476 mechanisms underlying the generation of ES, therefore, further studies are  
477 needed to elucidate its pathophysiology.

## 478 Figure Legends

479 Fig. 1. Results of magnetoencephalography (MEG), F-18-fluorodeoxyglucose  
480 positron emission tomography (FDG-PET), and invasive functional brain  
481 mapping.

482 A: Interictal analysis of spike-and-waves using MEG revealing three clusters of  
483 dipoles in the right frontal, parietal, and temporal association cortices (dipoles  
484 with goodness of fit  $\geq 80\%$ ).

485 B: FDG-PET showing hypometabolism in regions corresponding to the clusters of  
486 MEG dipoles.

487 C: Subdural electrode placement superimposed on the pre-operative MRI image  
488 and co-registered with the post-implanted MRI image. Functional brain mapping  
489 was performed using high-frequency (50 Hz) electrical stimulation and the  
490 normal functional configuration of the positive motor area was confirmed.

491 Resection areas are shown with red frames.

492 Abbreviations: A, anterior; P, posterior; R, right; L, left; CS, central sulcus; IFS,  
493 inferior frontal sulcus; IPS, intraparietal sulcus; PoCS, postcentral sulcus; PrCS,  
494 precentral sulcus; SFS, superior frontal sulcus; Sylv, sylvian fissure; U/E, upper  
495 extremities.

496

497 Fig. 2. CCEP data acquisition.

498 (A) Repetitive SPES was applied to nine pairs of electrodes at the PMA (PMA:  
499 blue frame). Representative CCEP waveforms are shown by stimulating one of  
500 the PMA electrode pairs. CCEPs showed a relatively limited response in the PMA  
501 (yellow). The vertical line corresponds to the time of the stimulation (white

502 arrowhead). The time window was 600 ms in duration (-100 to +500 ms, relative  
503 to SPES onset) and the baseline was set using a 95 ms period (-100 to -5 ms  
504 relative to SPES onset). The number of significant CCEP electrodes was 16  
505 (yellow) at the PMA and 114 at the whole cortical areas covered by the subdural  
506 grid, yielding the index ratio of 14.0%.

507 (B) Repetitive SPES was applied to sixty-two pairs of electrodes that were  
508 located in non-PMA (frontal, 30 pairs; temporal, 18 pairs; parietal, 14 pairs).  
509 Representative CCEP waveforms are shown by stimulating an electrode pair in  
510 the inferior parietal lobule, which was one of the seizure onset zones included in  
511 the resection areas (red frames). CCEPs showed the cortico-cortical connectivity  
512 to the frontal lobe across the central sulcus and the temporal lobe, relatively  
513 sparing the PMA (green). The number of significant CCEP electrodes at PMA  
514 was 11 (green) and that at the whole cortical areas covered by the subdural grid  
515 was 101, yielding the index ratio of 10.9%.

516 (C) The magnified time-course of the representative channel in Fig.2B. One of  
517 the channels in the frontal lobe showed a significant response, with N1 amplitude  
518 greater than 6 SD above the baseline (-100 to -5 ms, relative to SPES onset).

519 (D) Comparison of the index ratio between the PMA and non-PMA stimulation.  
520 The index ratio is defined by dividing the number of significant CCEP electrodes  
521 at PMA by that at the whole cortical areas covered by subdural electrodes. The  
522 index ratio of PMA stimulation ( $16.1 \pm 4.8\%$ ) was higher than that of non-PMA  
523 stimulation (non-PMA:  $12.3 \pm 5.9\%$ ) (Wilcoxon signed-rank test with correction  
524 for multiple comparisons,  $p < 0.05$ ).

525 Abbreviations: CCEP, cortico-cortical evoked potential; SPES, single pulse

electrical stimulation; CS, central sulcus; IFS, inferior frontal sulcus; IPS, intraparietal sulcus; positive motor area; PMA; PoCS, postcentral sulcus; PrCS, precentral sulcus; SFS, superior frontal sulcus; Sylv, sylvian fissure.

Fig. 3. Analysis of EEG with functional MRI (EEG-fMRI) results.

A: Two examples of identified interictal epileptiform discharges (gray frame).

Total recording time was 60 min and the number of analyzed spike-and-waves was 228.

B: EEG-fMRI findings. EEG-fMRI analysis with time-shift models (-4 to +4 s)

revealing spike-and-wave-related activation in subcortical structures

(predominantly right bilateral thalamus, and midbrain) and in right-dominant

bilateral frontal, temporal, and parietal lobes, sparing the positive motor area.

Activation is also observed in left-dominant bilateral cerebellum. The bilateral

positive motor area, superior parietal lobule, and precuneus show negative

BOLD activity (deactivation; 0 to +4 s). The Z-statistic image threshold at  $Z > 2.3$

at the voxel level to identify clusters, with the corrected cluster significance level

was set at  $p < 0.007$ .

Abbreviations: BOLD, blood-oxygen-level-dependent; t, time; A, anterior; P,

posterior; R, right; L, left.

Fig. 4. Time-frequency representation of ictal HFOs from a representative ES

event.

The time of onset of EMG changes in the left deltoid muscle was set to 0

s. The spectral power ( $\mu V^2$ ) was computed for the given frequency range and

550 window with reference to the baseline activity (-2.5 to -1.5 s, relative to EMG  
551 onset). The spectrogram shows that HFOs (mainly of 80–120 Hz) started prior to  
552 the onset of EMG in the majority of electrodes. Ictal HFOs were widely  
553 distributed, mainly in the anterior frontal and parietal lobes. These areas were  
554 subsequently resected (red frames), initially sparing the positive motor area  
555 (blue frame). Spectrogram: vertical frequency range, 0–500 Hz; color scale  
556 (logarithmic), -5 to +5 B; baseline, -2.5 to -1.5 s relative to EMG onset.  
557 Abbreviations: CS, central sulcus; IFS, inferior frontal sulcus; IPS, intraparietal  
558 sulcus; PoCS, postcentral sulcus; PrCS, precentral sulcus; SFS, superior frontal  
559 sulcus; Sylv, sylvian fissure; EMG, electromyogram.

560

561 Fig. 5. Analyses of ictal HFOs.

562 (A) Maximal power in the ripple band (80–250 Hz) of each lobe in the first ES  
563 from each of the six clusters.

564 First, the mean power was calculated in the ripple band (80–250 Hz) from -2.5 to  
565 -1.5 s as the baseline of the logarithmic scale. The power changes of the time  
566 segment from -1.5 to +2.5 s relative to each first ES compared to the mean power  
567 were subsequently analyzed. The maximal power of each electrode was  
568 calculated and frontal cortex (60 electrodes), positive motor area (18 electrodes),  
569 parietal cortex (28 electrodes), and temporal cortex (42 electrodes) were  
570 compared. The power of frontal, parietal, and temporal were significantly higher  
571 than those in the positive motor area (\*Wilcoxon signed-rank test with correction  
572 for multiple comparisons,  $p < 0.05$ ). Data points shown (X), were derived from  
573 the analysis of the first ES from each of the six clusters.

574 (B) Time at which power exceeded the mean + 3 SD.

575 Instances at which the power exceeded the mean + 3 SD were detected and their  
 576 timing compared between lobes. Instances at which the power exceeded the  
 577 mean + 3 SD in frontal, parietal, and temporal occurred significantly earlier than  
 578 those in the positive motor area (\*Wilcoxon signed-rank test with correction for  
 579 multiple comparisons,  $p < 0.05$ ). Data points shown ( $\circ$ ) were derived from the  
 580 analysis of first ES from each of the six clusters.

581

582 Fig. 6. Schematics of potential mechanisms underlying the generation of ES in  
 583 the patient.

584 (A) Distribution of EEG-fMRI activations.

585 EEG-fMRI revealing spike-and-wave-related activation in right-dominant bilateral  
 586 frontal (red), temporal (yellow), and parietal lobes (green), sparing the PMA.  
 587 Activation is also observed in the cerebellum (orange). The intensity of each  
 588 color indicates the degree of EEG-fMRI activation.

589 (B) Distribution of ictal HFOs.

590 The rectangles indicate the locations of main subdural electrodes and some of  
 591 the strips placed in the right hemisphere. Ictal HFOs were widely distributed,  
 592 primarily in the frontal (red) and parietal lobes (green), initially sparing the  
 593 positive motor area. The intensity of each color indicates the spectral power.

594 C: Connectivity analysis using CCEPs.

595 CCEPs reveal bidirectional fronto-parietal connections between the seizure  
 596 onset zones in the frontal (red), parietal (green), and temporal lobes (yellow),  
 597 sparing the PMA. The intensity of each color indicates the magnitude of the

598 response to SPES.

599 (D) Potential mechanisms underlying the generation of ES in the patient.

600 The cortico-reticulospinal tract consists of the CRT (black line) and reticulospinal  
601 tract (RST; gray and dashed gray lines). Potential mechanisms underlying the  
602 generation of ES in this patient involve abnormal impulses involving the premotor  
603 cortex (red), which is well-connected with the temporal (yellow) and parietal and  
604 occipital lobes (green), with the exception of the PMA. The impulses descend  
605 through the CRT to the medullary reticular formation, and are transmitted via the  
606 dorsal RST. An imbalance in signaling in the medial and dorsal RST may be  
607 responsible for the abnormal activation of axial and proximal muscles in the  
608 extremities, leading to ES. Abbreviations: (+), facilitation; (-), inhibition; CRT,  
609 corticoreticular tract; RST, reticulospinal tract; CS, central sulcus; IFS, inferior  
610 frontal sulcus; IPS, intraparietal sulcus; PMA, positive motor area; PoCS,  
611 postcentral sulcus; PrCS, precentral sulcus; SFS, superior frontal sulcus; Sylv,  
612 sylvian fissure.

613

614 Supplementary Fig. 1

615 Representative CCEP connectivity findings among the seizure onset zones in the  
616 association areas.

617 In addition to Fig 2B, where the CCEP connectivity findings are shown by  
618 stimulating one of the seizure onset zones in the inferior parietal lobule, SPES  
619 was applied to a pair of electrode in the seizure onset zones in the frontal (A) and  
620 temporal (B) areas. For both stimulation, a relatively limited but distinct response  
621 (marked with an asterisk) was observed in the seizure onset zone in the inferior

622 parietal lobule, where the stimulus is delivered in Fig 2B. CCEP investigation  
623 showed the bidirectional cortico-cortical connectivity across the central sulcus,  
624 relatively sparing the PMA, among the seizure onset zones in the association  
625 area. Note responses in the PMA were not evident (index ratio was 12.1% and  
626 7.1%, respectively). The vertical line corresponds to the time of the stimulation  
627 (white arrowhead). The time window was 600 ms in duration (-100 to +500 ms,  
628 relative to SPES onset) and the baseline was set using a 95 ms period (-100 to -5  
629 ms relative to SPES onset).



## 630 References

- 631 Aghakhani Y, Bagshaw AP, Benar CG, Hawco C, Andermann F, Dubeau F, et al.  
632 fMRI activation during spike and wave discharges in idiopathic generalized  
633 epilepsy. *Brain*. 2004;127:1127-44.
- 634 Akiyama T, Chan DW, Go CY, Ochi A, Elliott IM, Donner EJ, et al. Topographic  
635 movie of intracranial ictal high-frequency oscillations with seizure semiology:  
636 epileptic network in Jacksonian seizures. *Epilepsia*. 2011;52:75-83.
- 637 Amiri M, Lina JM, Pizzo F, Gotman J. High Frequency Oscillations and spikes:  
638 Separating real HFOs from false oscillations. *Clin Neurophysiol*.  
639 2016;127:187-96.
- 640 Avoli M, Rogawski MA, Avanzini G. Generalized epileptic disorders: an update.  
641 *Epilepsia*. 2001;42:445-57.
- 642 Behrens TE, Johansen-Berg H, Woolrich MW, Smith SM, Wheeler-Kingshott CA,  
643 Boulby PA, et al. Non-invasive mapping of connections between human thalamus  
644 and cortex using diffusion imaging. *Nat Neurosci*. 2003;6:750-7.
- 645 Benar CG, Chauviere L, Bartolomei F, Wendling F. Pitfalls of high-pass filtering  
646 for detecting epileptic oscillations: a technical note on "false" ripples. *Clin*  
647 *Neurophysiol*. 2010;121:301-10.
- 648 Bragin A, Engel J, Jr., Staba RJ. High-frequency oscillations in epileptic brain.  
649 *Curr Opin Neurol*. 2010;23:151-6.
- 650 Bragin A, Engel J, Jr., Wilson CL, Fried I, Buzsaki G. High-frequency oscillations  
651 in human brain. *Hippocampus*. 1999;9:137-42.
- 652 Casey BJ, Tottenham N, Liston C, Durston S. Imaging the developing brain: what  
653 have we learned about cognitive development? *Trends Cogn Sci*. 2005;9:104-10.

- 654 Catani M, de Schotten MT. Projection Systems. Atlas of human brain connections.  
655 New York: Oxford University Press; 2012. p.379-96.
- 656 Chugani HT, Ilyas M, Kumar A, Juhasz C, Kupsky WJ, Sood S, et al. Surgical  
657 treatment for refractory epileptic spasms: The Detroit series. *Epilepsia*.  
658 2015;56:1941-9.
- 659 Chugani HT, Shewmon DA, Sankar R, Chen BC, Phelps ME. Infantile spasms: II.  
660 Lenticular nuclei and brain stem activation on positron emission tomography.  
661 *Ann Neurol*. 1992;31:212-9.
- 662 Deoni SC, Dean DC, 3rd, O'Muircheartaigh J, Dirks H, Jerskey BA. Investigating  
663 white matter development in infancy and early childhood using myelin water  
664 fraction and relaxation time mapping. *Neuroimage*. 2012;63:1038-53.
- 665 Engel J. A proposed diagnostic scheme for people with epileptic seizures and  
666 with epilepsy: report of the ILAE Task Force on Classification and Terminology.  
667 *Epilepsia*. 2001;42:796-803.
- 668 Fisher RS, Cross JH, French JA, Higurashi N, Hirsch E, Jansen FE, et al.  
669 Operational classification of seizure types by the International League Against  
670 Epilepsy: Position Paper of the ILAE Commission for Classification and  
671 Terminology. *Epilepsia*. 2017;58:522-30.
- 672 Flechsig P. Developmental (myelogenetic) localisation of the cerebral cortex in  
673 the human subject. *Lancet*. 1901;158:1027-30.
- 674 Frauscher B, Bartolomei F, Kobayashi K, Cimbalnik J, van 't Klooster MA, Rampp  
675 S, et al. High-frequency oscillations: The state of clinical research. *Epilepsia*.  
676 2017;58:1316-29.
- 677 Gotman J, Grova C, Bagshaw A, Kobayashi E, Aghakhani Y, Dubeau F.

678 Generalized epileptic discharges show thalamocortical activation and  
679 suspension of the default state of the brain. *Proc Natl Acad Sci U S A*.  
680 2005;102:15236-40.

681 Hamandi K, Salek-Haddadi A, Laufs H, Liston A, Friston K, Fish DR, et al.  
682 EEG-fMRI of idiopathic and secondarily generalized epilepsies. *Neuroimage*.  
683 2006;31:1700-10.

684 Imura Y, Jones K, Hattori K, Okazawa Y, Noda A, Hoashi K, et al. Epileptogenic  
685 high-frequency oscillations skip the motor area in children with multilobar  
686 drug-resistant epilepsy. *Clin Neurophysiol*. 2017;128:1197-205.

687 Imura Y, Jones K, Takada L, Shimizu I, Koyama M, Hattori K, et al. Strong  
688 coupling between slow oscillations and wide fast ripples in children with epileptic  
689 spasms: Investigation of modulation index and occurrence rate. *Epilepsia*.  
690 2018;59:544-54.

691 Imamura H, Matsumoto R, Inouchi M, Matsushashi M, Mikuni N, Takahashi R, et al.  
692 Ictal wideband ECoG: direct comparison between ictal slow shifts and high  
693 frequency oscillations. *Clin Neurophysiol*. 2011;122:1500-4.

694 Jacobs J, Staba R, Asano E, Otsubo H, Wu JY, Zijlmans M, et al. High-frequency  
695 oscillations (HFOs) in clinical epilepsy. *Prog Neurobiol*. 2012;98:302-15.

696 Jacobs J, Zijlmans M, Zelmann R, Chatillon CE, Hall J, Olivier A, et al.  
697 High-frequency electroencephalographic oscillations correlate with outcome of  
698 epilepsy surgery. *Ann Neurol*. 2010;67:209-20.

699 Japaridze N, Muthuraman M, Moeller F, Boor R, Anwar AR, Deuschl G, et al.  
700 Neuronal networks in west syndrome as revealed by source analysis and  
701 renormalized partial directed coherence. *Brain Topogr*. 2013;26:157-70.

702 Jiruska P, Alvarado-Rojas C, Schevon CA, Staba R, Stacey W, Wendling F, et al.  
703 Update on the mechanisms and roles of high-frequency oscillations in seizures  
704 and epileptic disorders. *Epilepsia*. 2017;58:1330-9.

705 Jiruska P, Powell AD, Chang WC, Jefferys JG. Electrographic high-frequency  
706 activity and epilepsy. *Epilepsy Res*. 2010;89:60-5.

707 Kably B, Drew T. Corticoreticular pathways in the cat. I. Projection patterns and  
708 collaterization. *J Neurophysiol*. 1998;80:389-405.

709 Kanazawa K, Matsumoto R, Imamura H, Matsushashi M, Kikuchi T, Kunieda T, et  
710 al. Intracranially recorded ictal direct current shifts may precede high frequency  
711 oscillations in human epilepsy. *Clin Neurophysiol*. 2015;126:47-59.

712 Keller CJ, Bickel S, Entz L, Ulbert I, Milham MP, Kelly C, et al. Intrinsic functional  
713 architecture predicts electrically evoked responses in the human brain.  
714 *Proceedings of the National Academy of Sciences*. 2011;108:10308-13.

715 Kobayashi K, Matsumoto R, Matsushashi M, Usami K, Shimotake A, Kunieda T, et  
716 al. High frequency activity overriding cortico-cortical evoked potentials reflects  
717 altered excitability in the human epileptic focus. *Clin Neurophysiol*.  
718 2017;128:1673-81.

719 Le Van Quyen M, Bragin A. Analysis of dynamic brain oscillations:  
720 methodological advances. *Trends Neurosci*. 2007;30:365-73.

721 Liu Y, Yang T, Liao W, Yang X, Liu I, Yan B, et al. EEG-fMRI study of the ictal and  
722 interictal epileptic activity in patients with eyelid myoclonia with absences.  
723 *Epilepsia*. 2008;49:2078-86.

724 Lüders H, Schule S, McIntyre C. General principles of cortical mapping by  
725 electrical stimulation. In: Lüders H, editor. *Textbook of epilepsy surgery*. New

- 726 York: CRC Press; 2008. p. 963–77.
- 727 Matsumoto R, Kunieda T, Nair D. Single pulse electrical stimulation to probe  
728 functional and pathological connectivity in epilepsy. *Seizure*. 2017;44:27-36.
- 729 Matsumoto R, Nair DR, LaPresto E, Bingaman W, Shibasaki H, Luders HO.  
730 Functional connectivity in human cortical motor system: a cortico-cortical evoked  
731 potential study. *Brain*. 2007;130:181-97.
- 732 Matsumoto R, Nair DR, Ikeda A, Fumuro T, Lapresto E, Mikuni N, et al.  
733 Parieto-frontal network in humans studied by cortico-cortical evoked potential.  
734 *Hum Brain Mapp*. 2012;33:2856-72.
- 735 Matsumoto R, Nair DR, LaPresto E, Najm I, Bingaman W, Shibasaki H, et al.  
736 Functional connectivity in the human language system: a cortico-cortical evoked  
737 potential study. *Brain*. 2004;127:2316-30.
- 738 Matsuyama K, Mori F, Nakajima K, Drew T, Aoki M, Mori S. Locomotor role of the  
739 corticoreticular–reticulospinal–spinal interneuronal system. *Prog Brain Res*.  
740 2004;143:239-49.
- 741 Moeller F, Stephani U, Siniatchkin M. Simultaneous EEG and fMRI recordings  
742 (EEG-fMRI) in children with epilepsy. *Epilepsia*. 2013;54:971-82.
- 743 Morel A, Magnin M, Jeanmonod D. Multiarchitectonic and stereotactic atlas of  
744 the human thalamus. *J Comp Neurol*. 1997;387:588-630.
- 745 Nariai H, Nagasawa T, Juhasz C, Sood S, Chugani HT, Asano E. Statistical  
746 mapping of ictal high-frequency oscillations in epileptic spasms. *Epilepsia*.  
747 2011;52:63-74.
- 748 Ochi A, Otsubo H, Donner EJ, Elliott I, Iwata R, Funaki T, et al. Dynamic changes  
749 of ictal high-frequency oscillations in neocortical epilepsy: using multiple band

750 frequency analysis. *Epilepsia*. 2007;48:286-96.

751 Ramachandranair R, Ochi A, Imai K, Benifla M, Akiyama T, Holowka S, et al.

752 Epileptic spasms in older pediatric patients: MEG and ictal high-frequency

753 oscillations suggest focal-onset seizures in a subset of epileptic spasms.

754 *Epilepsy Res*. 2008;78:216-24.

755 Siniatchkin M, van Baalen A, Jacobs J, Moeller F, Moehring J, Boor R, et al.

756 Different neuronal networks are associated with spikes and slow activity in

757 hypsarrhythmia. *Epilepsia*. 2007;48:2312-21.

758 Steriade M, Timofeev I. Generators of ictal and interictal electroencephalograms

759 associated with infantile spasms: intracellular studies of cortical and thalamic

760 neurons. *Int Rev Neurobiol*. 2002;49:77-98.

761 Uematsu S, Lesser R, Fisher RS, Gordon B, Hara K, Krauss GL, et al. Motor and

762 sensory cortex in humans: topography studied with chronic subdural stimulation.

763 *Neurosurgery*. 1992;31:59-72.

764 Usami K, Matsumoto R, Kobayashi K, Hitomi T, Matsuhashi M, Shimotake A, et al.

765 Phasic REM transiently approaches wakefulness in the human cortex—a

766 single-pulse electrical stimulation study. *Sleep*. 2017;40.

767 Usami K, Matsumoto R, Sawamoto N, Murakami H, Inouchi M, Fumuro T, et al.

768 Epileptic network of hypothalamic hamartoma: An EEG-fMRI study. *Epilepsy Res*.

769 2016;125:1-9.

770 Vigevano F, Fusco L, Pachatz C. Neurophysiology of spasms. *Brain Dev*.

771 2001;23:467-72.

772 Watanabe K, Negoro T, Okumura A. Symptomatology of infantile spasms. *Brain*

773 *Dev*. 2001;23:453-66.

- 774 Worsley, KJ. Statistical analysis of activation images. In: Jezzard P, Matthews  
775 PM, Smith SM, editors. Functional MRI: An Introduction to Methods. New York:  
776 Oxford University Press; 2001. p. 251–270.
- 777 Wu JY, Sankar R, Lerner JT, Matsumoto JH, Vinters HV, Mathern GW. Removing  
778 interictal fast ripples on electrocorticography linked with seizure freedom in  
779 children. *Neurology*. 2010;75:1686-94.
- 780 Yamao Y, Matsumoto R, Kunieda T, Arakawa Y, Kobayashi K, Usami K, et al.  
781 Intraoperative dorsal language network mapping by using single-pulse electrical  
782 stimulation. *Hum Brain Mapp*. 2014;35:4345-61.
- 783 Yeo SS, Chang MC, Kwon YH, Jung YJ, Jang SH. Corticoreticular pathway in the  
784 human brain: diffusion tensor tractography study. *Neurosci Lett*. 2012;508:9-12.
- 785 Zijlmans M, Worrell GA, Dimpelmann M, Stieglitz T, Barborica A, Heers M, et al.  
786 How to record high-frequency oscillations in epilepsy: A practical guideline.  
787 *Epilepsia*. 2017;58:1305-15.

Fig. 1

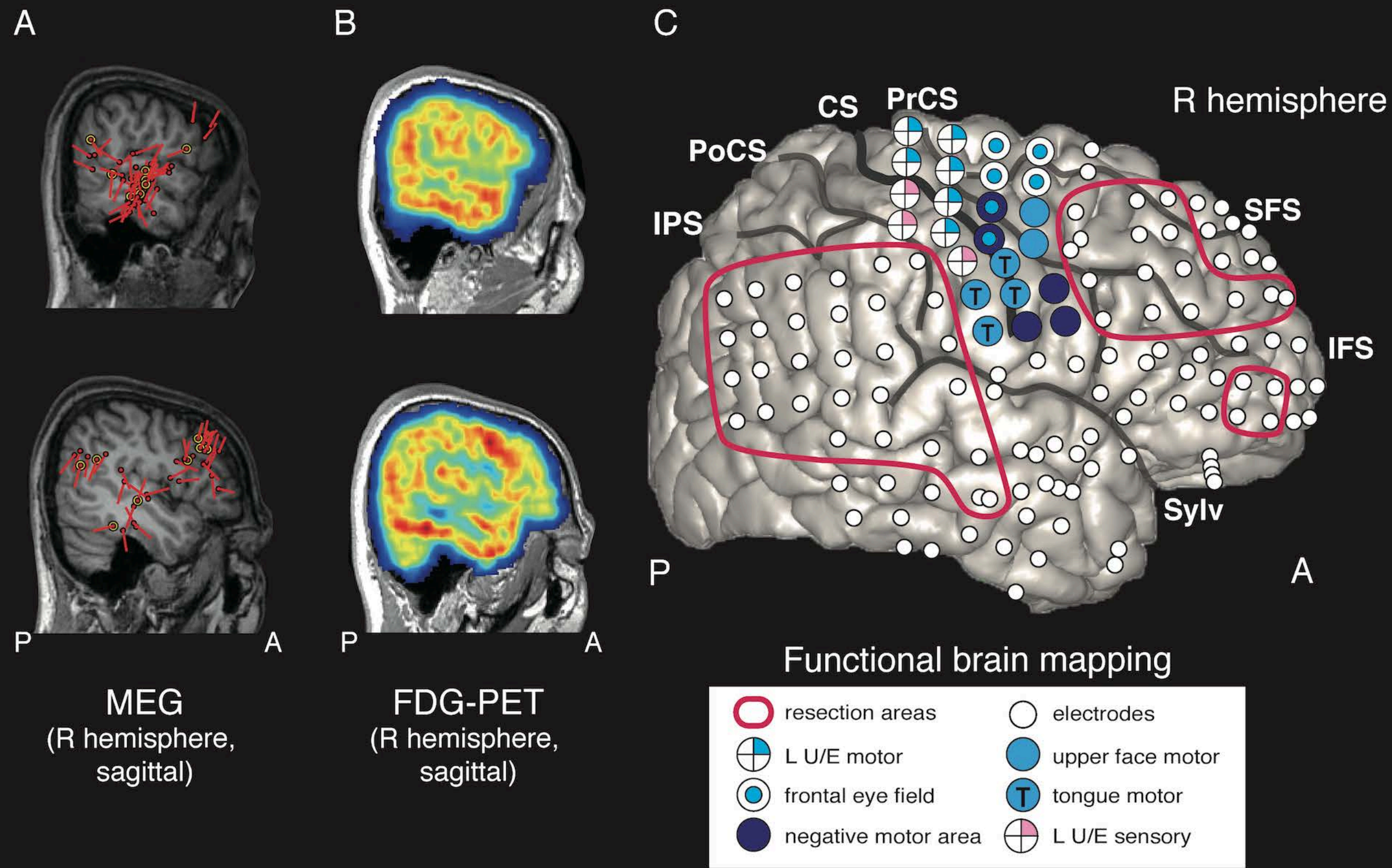
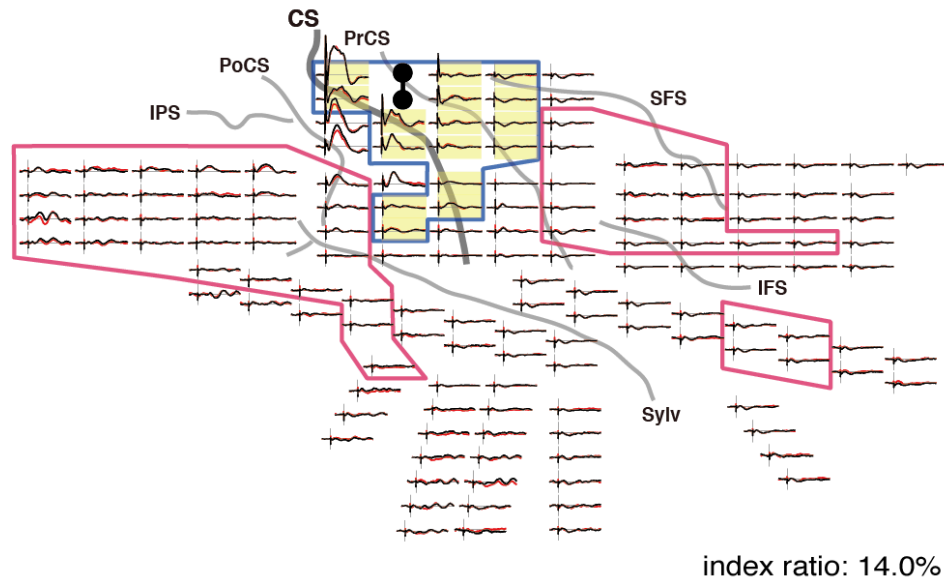


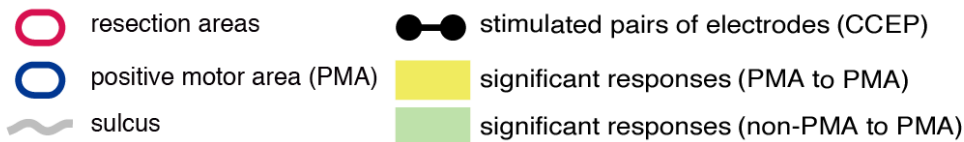
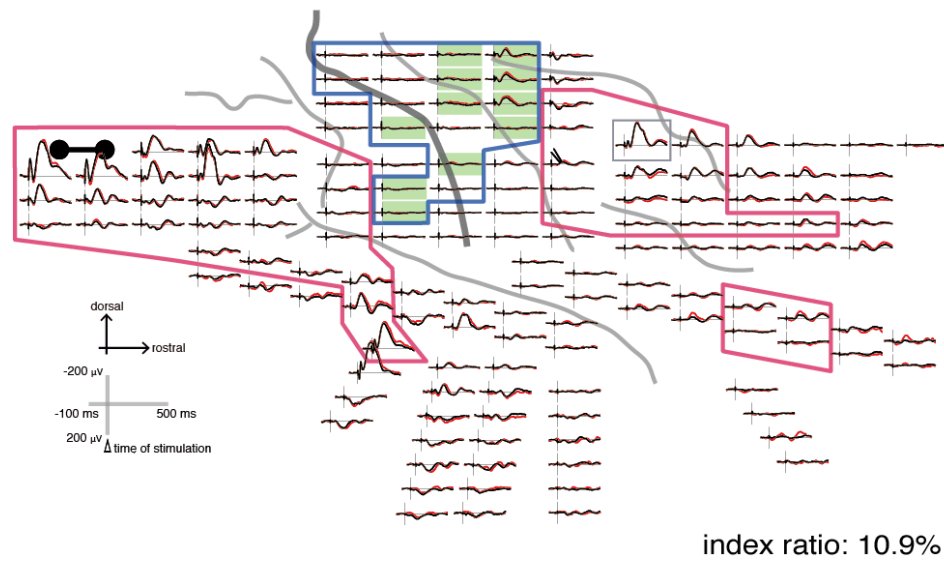


# Fig. 2

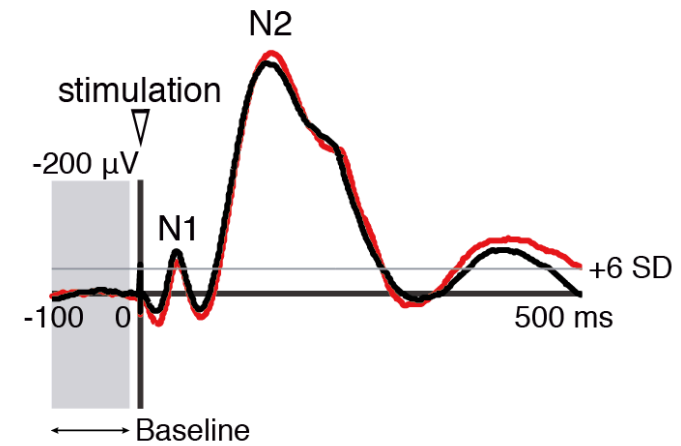
**A**



**B**



**C**



**D**

$$\text{index ratio} = \frac{\text{connections to PMA}}{\text{connections to all cortical regions covered by grid}} \times 100 (\%)$$

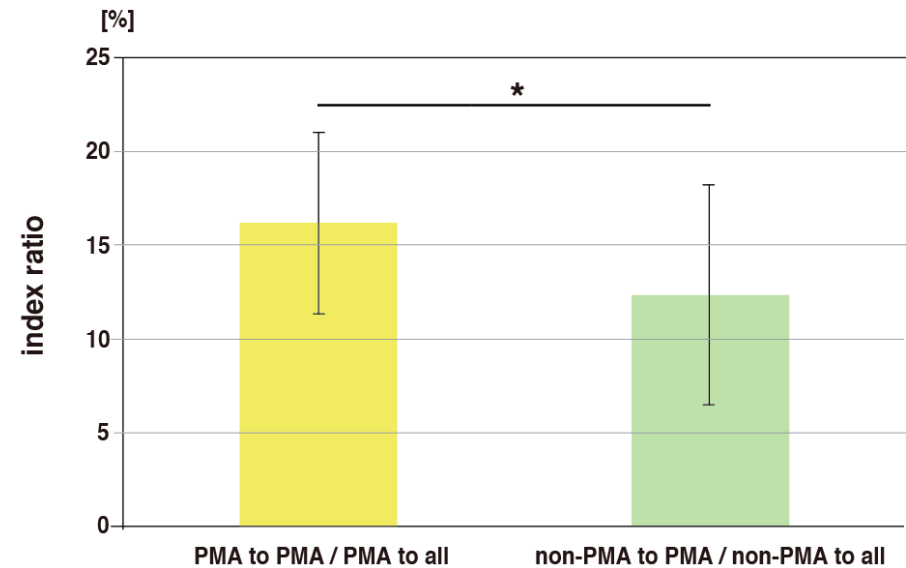
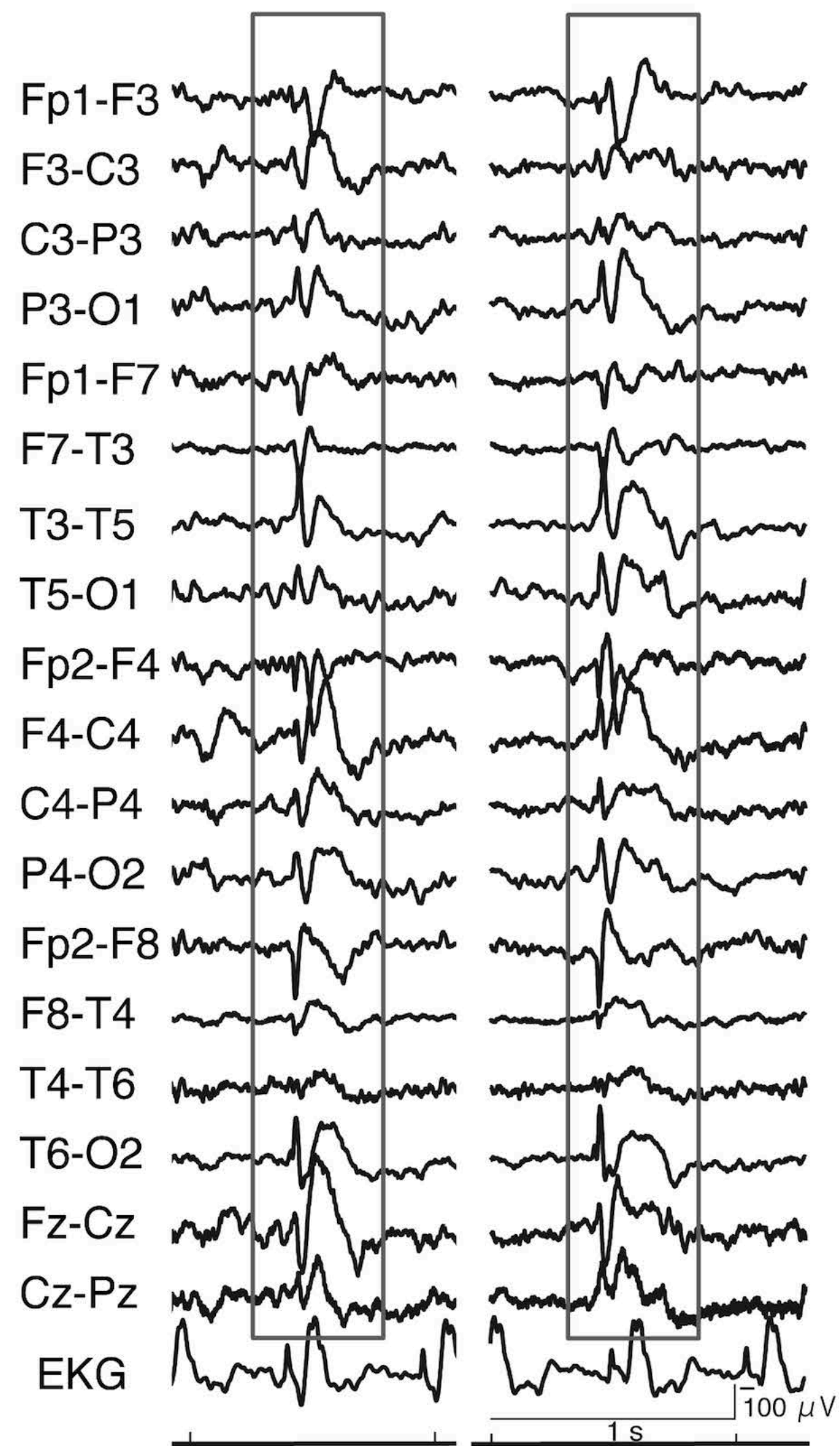




# Fig. 3

## A



## B

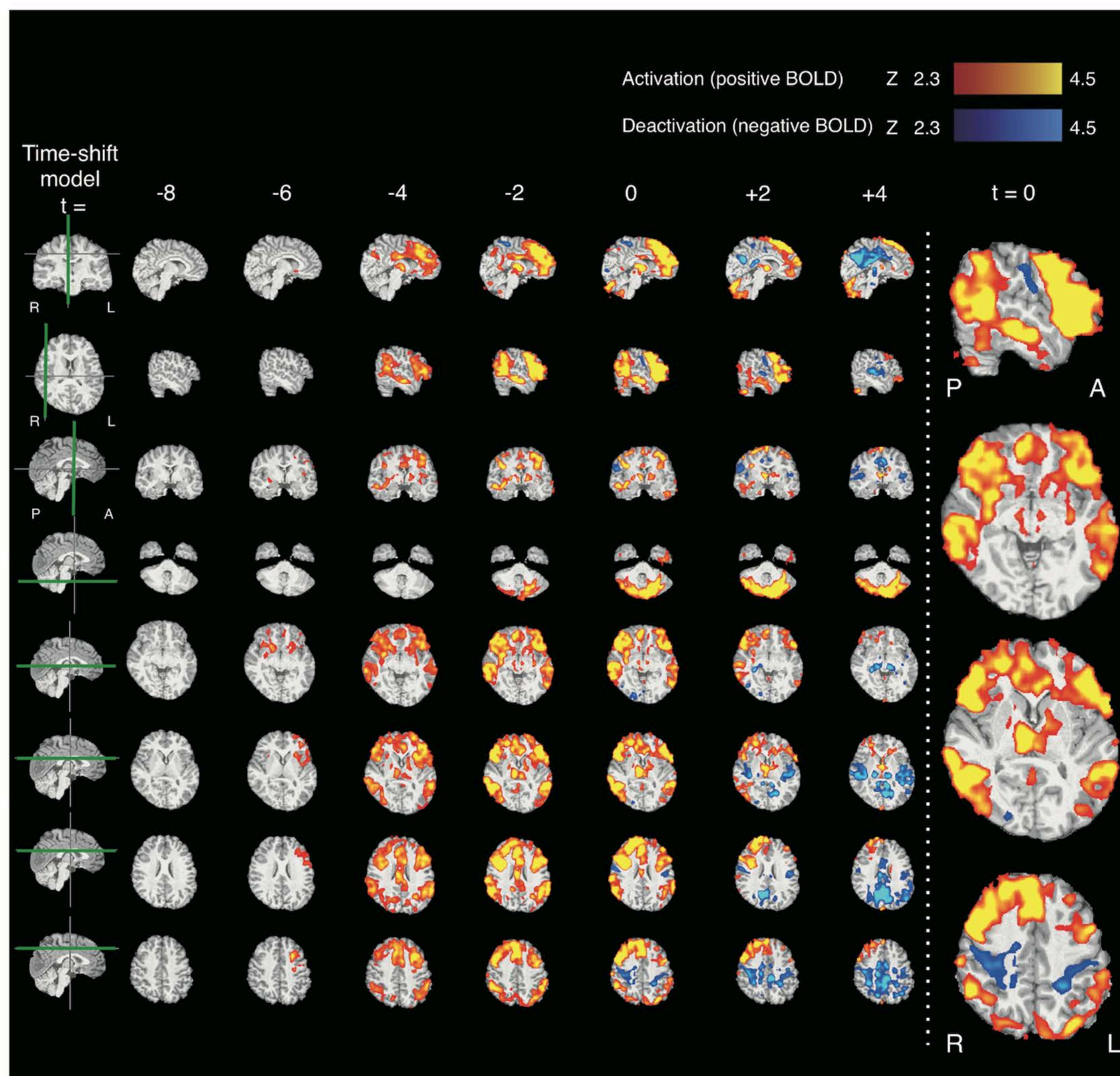




Fig. 4

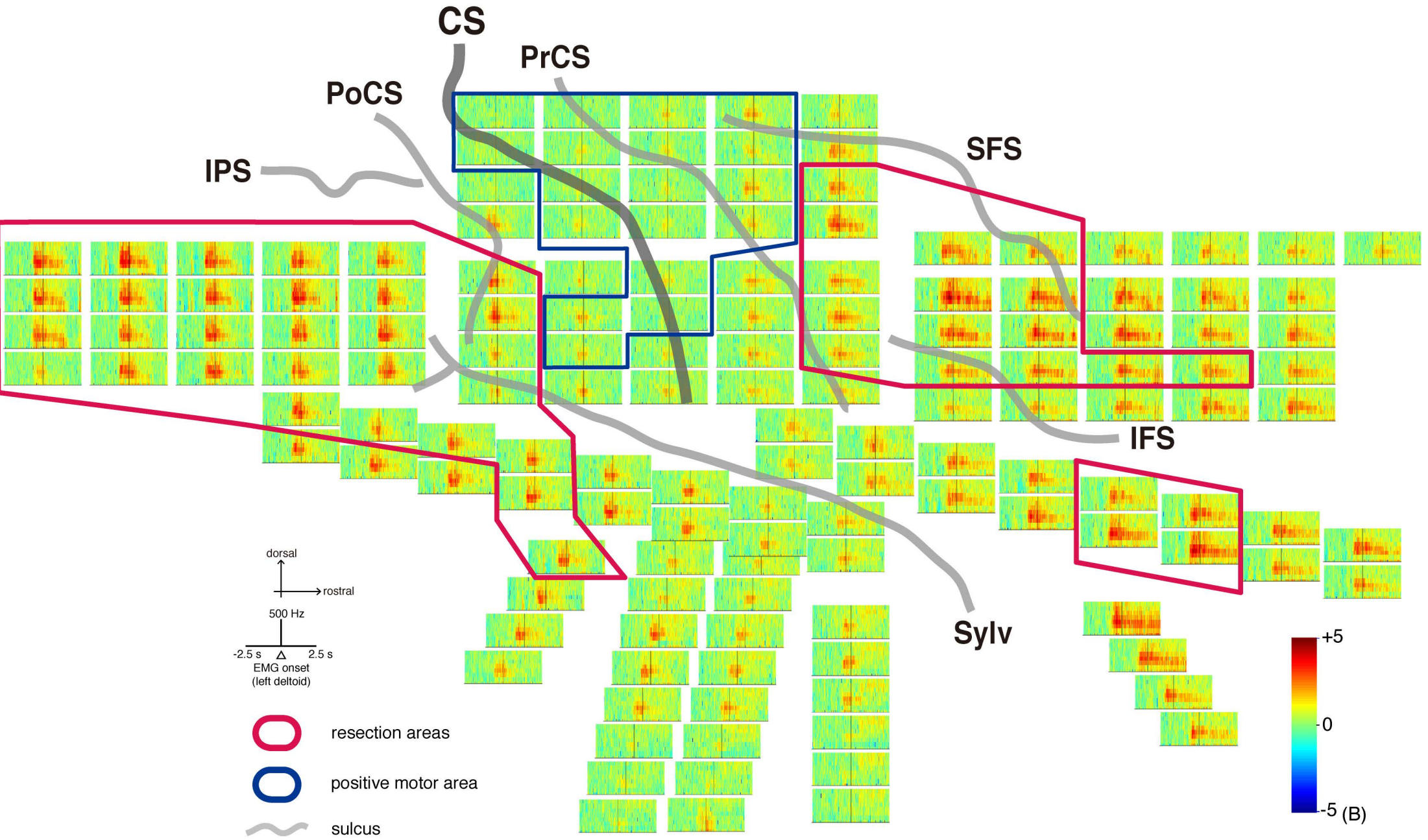


Fig. 5A

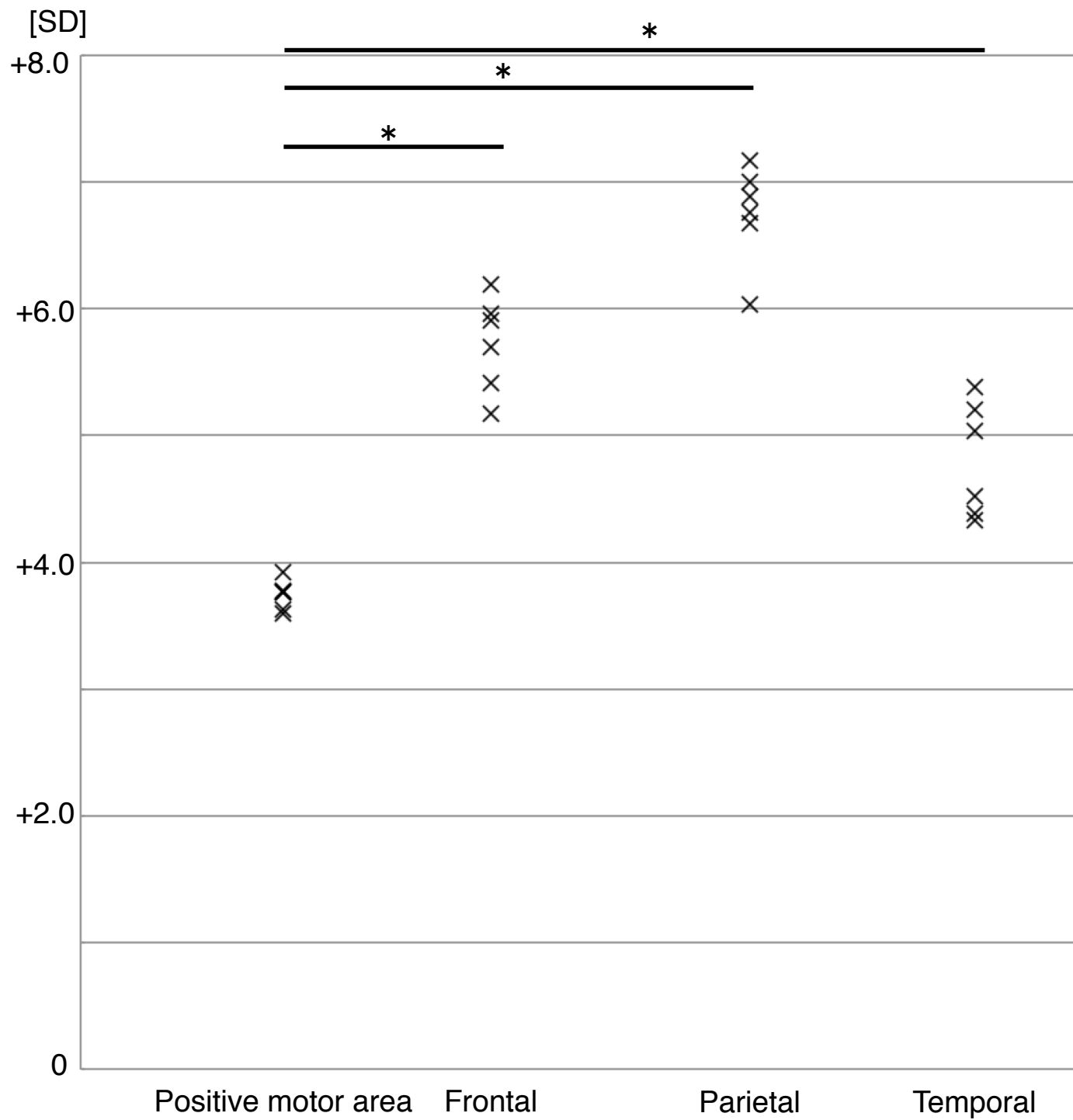
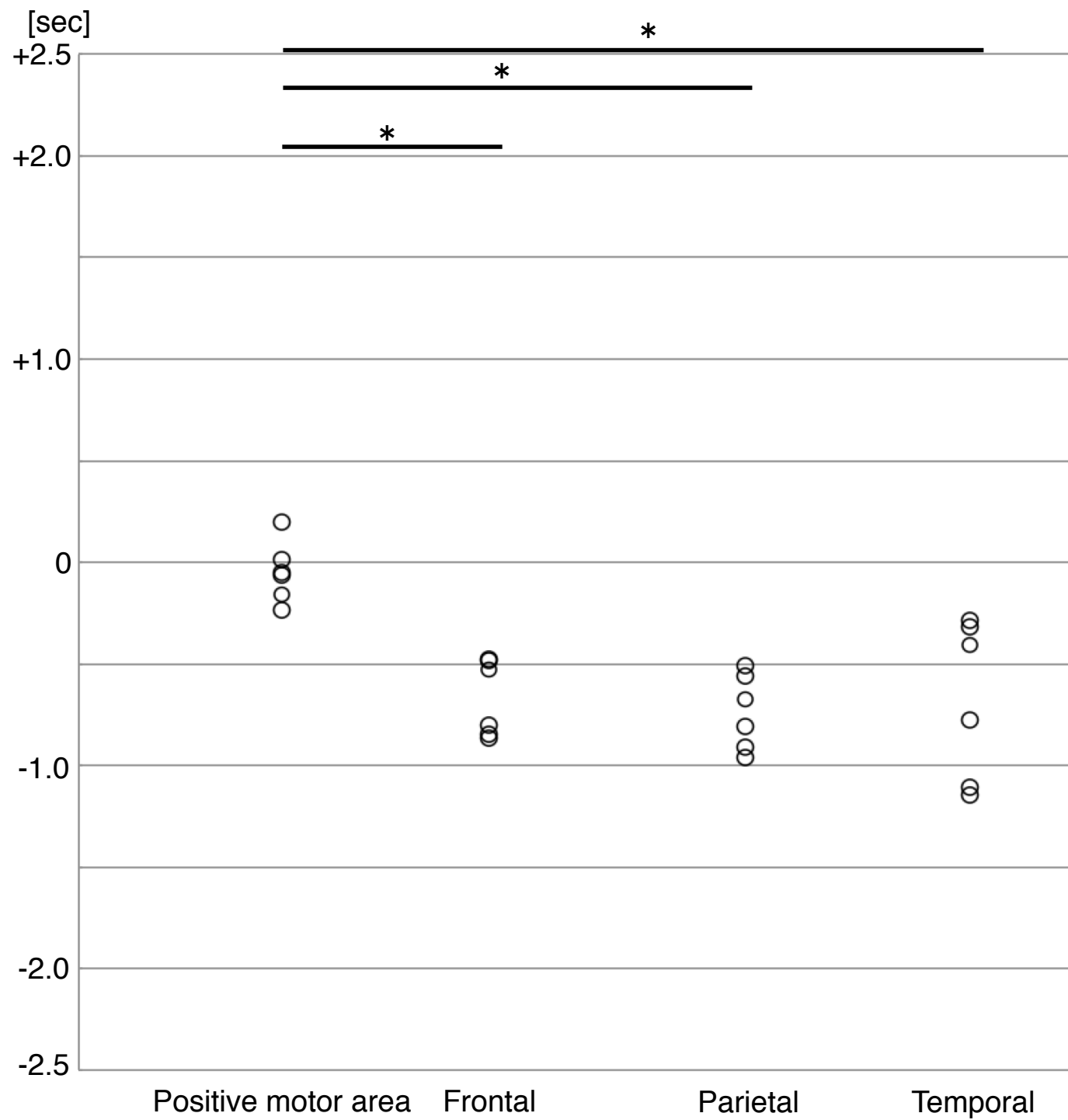
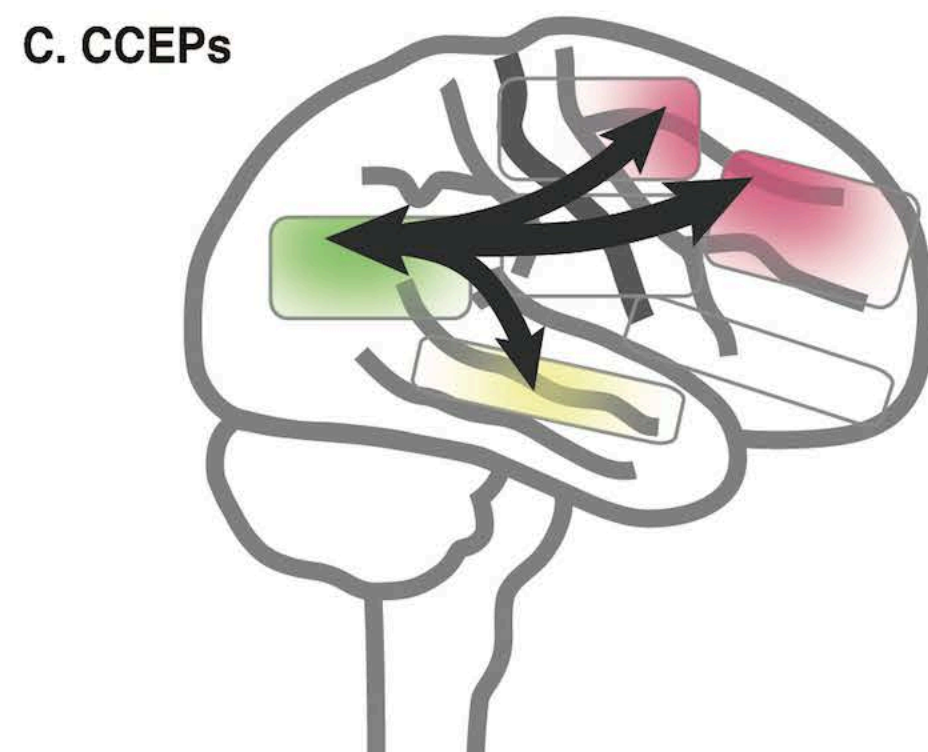
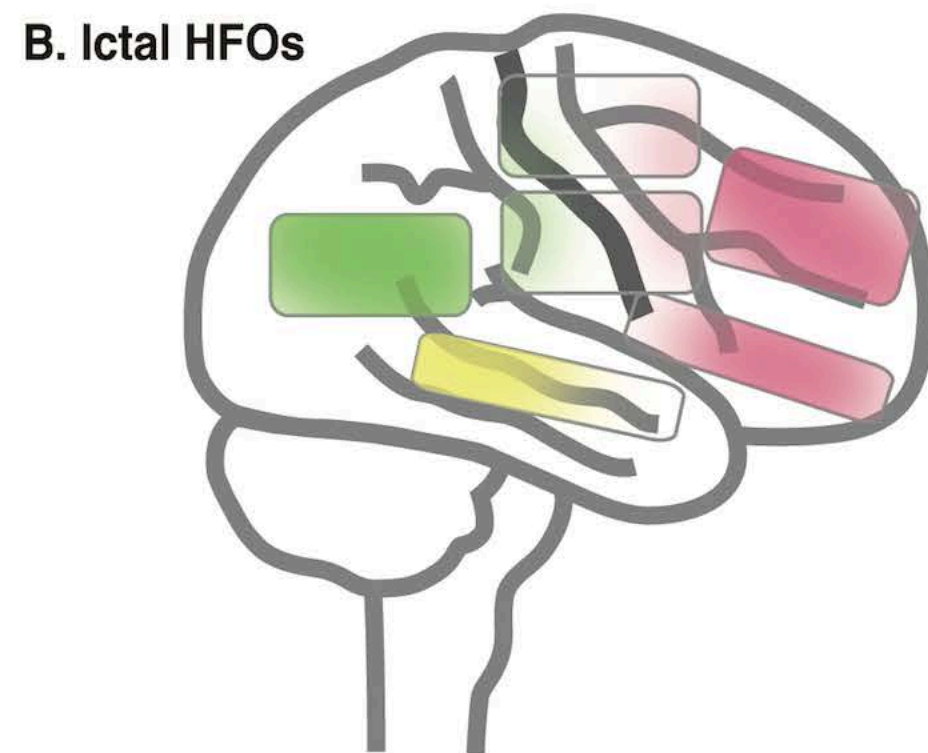
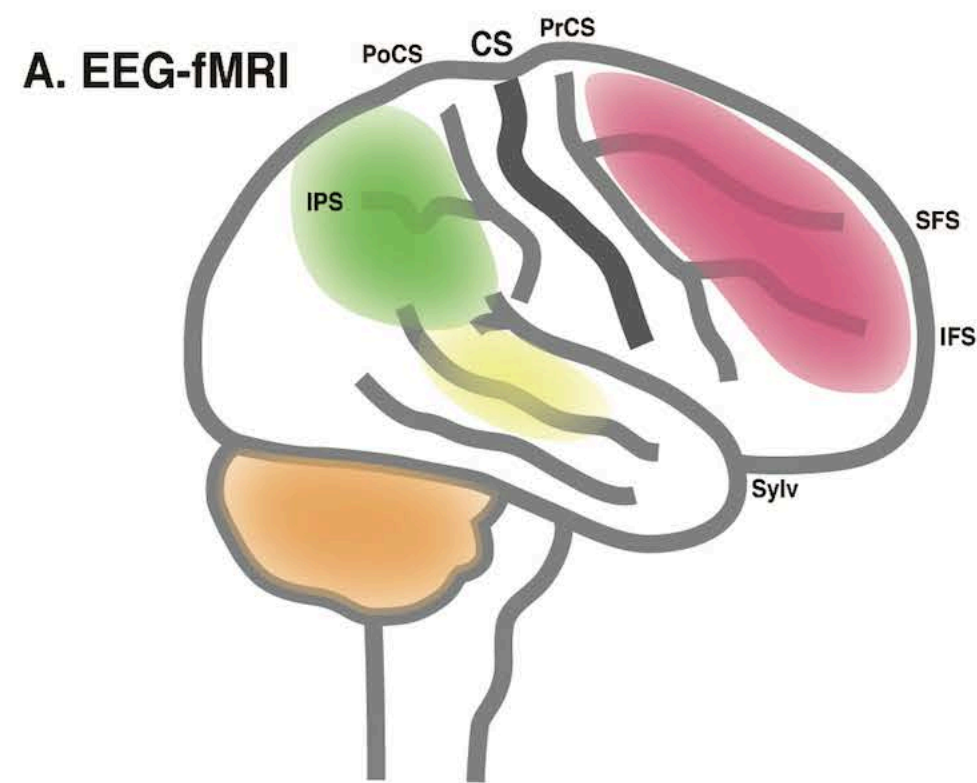


Fig. 5B

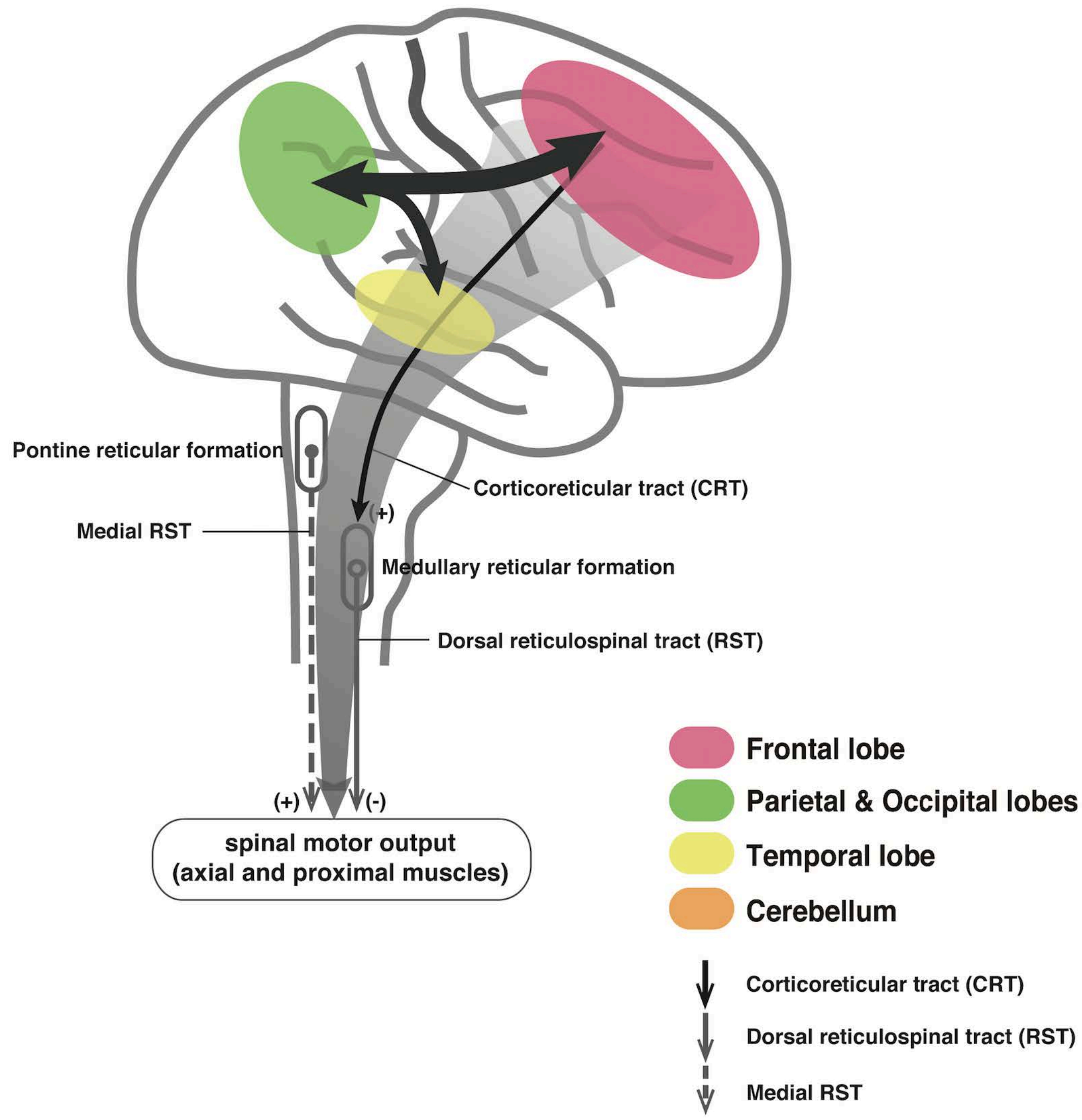




**Fig. 6**

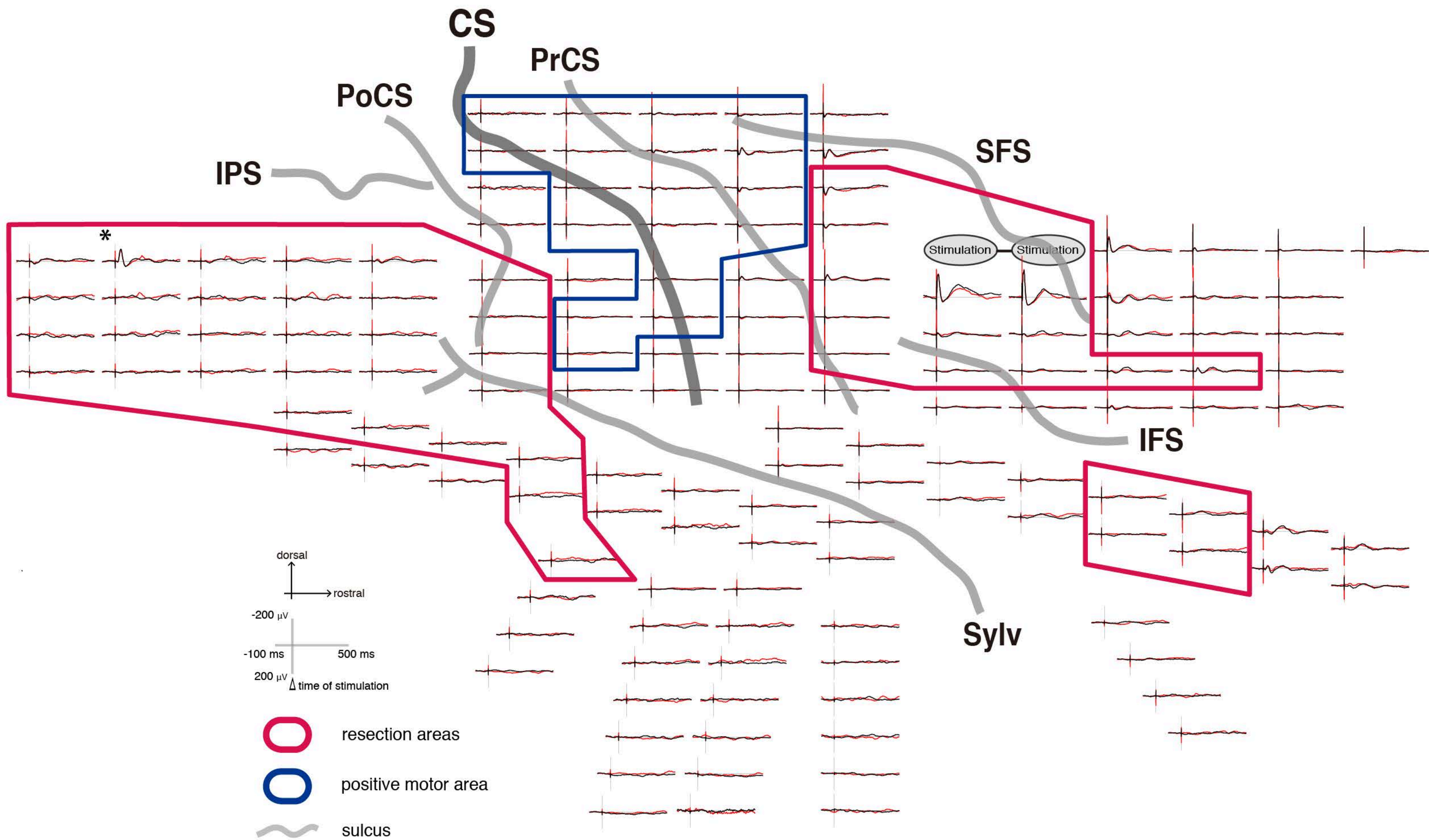


**D. Potential generator mechanism of epileptic spasms (in this patient)**





Supplementary Fig. 1A





Supplementary Fig. 1B

